INTERNATIONAL JOURNAL OF AUTOMOTIVE AND MECHANICAL ENGINEERING (IJAME)
ISSN: 2229-8649 e-ISSN: 2180-1606
VOL. 18, ISSUE 2, 8714 – 8727
DOI: https://doi.org/10.15282/ijame.18.2.2021.09.0665

ORIGINAL ARTICLE

Effects of Bearing Steps on Probable Wear Damage of Main Bearings of an IC Engine

H. Karimaei[1*] and H.R. Chamani[2]

[1]Aerospace Research Institute, Ministry of Science, Research and Technology, Tehran 14668-834, Iran
Phone: +982188366030; Fax: +982188362011
[2]Faculty of Mechanical Engineering, Iran University of Science and Technology, Tehran 16846, Iran

ABSTRACT – When two bearing shells are assembled in the bearing housing, it is possible that the edges of the two shells do not fit in the radial direction completely and have an offset relative to each other. This assembly error, which can have different causes, is called the bearing step in this paper. The bearing step can lead to wear damage in bearings. The effects of bearing step on the lubrication performance of main bearings and the probable wear damage have been investigated. To calculate the bearing lubrication characteristics such as maximum oil film pressure and minimum oil film thickness, elasto-hydrodynamic model, which includes the mass conservation algorithm, has been applied. The objective of this work is to investigate the effects of bearing steps on the lubrication performance of the main bearings and assess the probable wear damage of main bearings due to bearing step. The prediction of elasto-hydrodynamic model is very proximate to what really happened. The results show that for the under-study 12-cyl engine, main bearing No. 2 involved with medium wear damage. Wear damage in this main bearing No. 3 is not a concern, while main bearing No.4, 5 and 6 do not predict the probability of wear damage. For main bearing No.7, it is concluded that considering step and bore relief in simulation has high importance so that the solution without step and bore relief does not predict the wear, but with step and bore relief predicts medium wear damage.

ARTICLE HISTORY
Received: 9th July 2020
Revised: 13th Mar 2021
Accepted: 15th June 2021

KEYWORDS
Bearing step;
Lubrication performance;
Main bearing;
Wear damage;
Elasto-hydrodynamic

NOMENCLATURE

E^*	composite elastic modulus
F	a factor depending on ratio of $\Delta = h/\sigma_s$
h	oil film thickness
K	elastic factor
p	pressure (unit:)
α	pressure viscosity coefficient
β	radius at asperity summit
θ	clearance fill ratio (unit: -)
v	Poisson's ratio of the contacting surfaces
σ_s	composite surface asperity height
η_0	viscosity at the ambient pressure
η_S	surface density peak on each surface
Subscript	
s	surface

INTRODUCTION

Cavitation and wear abrasion are prevalent damages in engine bearing shells. In the event of cavitation erosion, the bearing surface is locally damaged because the creation and prompt collapse of small gas bubbles lead to generating strong pressure pulses. Due to strong dynamic loading, oil flow turbulence, oscillation of pins and some other factors, cavitation failure is observed in the bearings of heavy-duty diesel engines. Regarding the other failure, which is wear, it should be noted that wear damage adjusts the bearing geometry and subsequently affects the oil film pressure and the bearing shell durability. In the literature, only a few studies have been conducted about bearing step on the lubrication characteristics, which are not mainly related to diesel engines, thus lacking detailed study on the effect of bearing step.

Ushijima et al. [1] applied a wear model for bearing similar to Archard [2] model. In his model, the reaction force from asperity contacts was involved in the wear calculation. The bearing wear increased at the edges of bearing length, and crack also observed near the edges. Wang et al. [3] derived the relation of wear volume and the change of average surface roughness with the assumption of no plastic deformation. The flattening of asperities on a rough engineering surface was simulated with numerical techniques to predict dynamic wear in run-in contacts under partial elasto-hydrodynamic conditions. Their proposed model was based on line contact condition and should be developed for 3D

*CORRESPONDING AUTHOR | H. Karimaei | ✉ karimaei@ari.ac.ir

contact condition. The simulated results showed that the variation of wear volume and the change of average roughness could be described by a second-order polynomial.

There are different traditional methods to calculate the main bearing load, as reviewed in [4] and [5]. Cho et al. [6], experimentally measured the main bearing force components of a four in-line engine, in vertical and horizontal directions, using two different ring type load cells mounted in each main bearing cap bolt. They compared the experimental results with the theoretical results obtained by the statically determination method. It is illustrated that the statically determination method is not in agreement with the experimental results. Pratik et al. [7] did a live case study of premature failure of a crankcase; selected as per the requirement of the user. This paper focuses on a critical survey of literature and uses methodologies to find out the critical area through static analysis. The analysis result validates the point of high stress where the crack was initiated. Analysis of crankshaft has also been performed, and its analysis proves to be safe in the given working conditions. Rozhdestvensky et al. [8] present the solution to the interconnected problem of main bearings dynamics for the forced internal combustion (IC) engine. It analyses not only the influence of macro geometry parameters of each main bearing and the influence of non-Newtonian properties of lubricant but also the elastic characteristics of a crankshaft and crankcase and supports displacements caused by thermal deformation of an engine crankcase.

Oil film lubrication analysis in big eye and main bearings of an IC engine was done by Chamani and Karimaei [9] using elasto-hydrodynamic technique. They showed that bearing deformation affect the bearing failure such as wear and fretting fatigue. Then, they studied cavitation and wear damages in connecting rod big eye bearing of an IC engine using elasto-hydrodynamic technique [10]. They considered two different connecting rod structures of an IC engine and investigated their effects on wear erosion. They parametrically studied the lubrication characteristics of oil film in big eye bearing of an IC engine using elasto-hydrodynamic technique and investigated the effects of different parameters. The results showed that oil temperature, rotational speed of the engine, bearing clearance and flexibility of connecting rod big eye have considerable effect on lubrication characteristics. They also predicted the wear damage in connecting rod big eye bearing of an IC engine using elasto-hydrodynamic analysis. Finally, Chamani et al. [11] implemented the thermo-elasto-hydrodynamic (TEHD) lubrication model in the big eye bearing of an IC engine and thus considered the influence of temperature. The results showed that the TEHD method estimates higher maximum oil film pressure and lower minimum oil film thicknesses.

Karimaei et al. [12] studied the effect of elastic deformations of both crankshaft and crankcase on the load distribution in the main bearings. According to the results, the load distribution on the engine main bearings and bearing shell deformation were affected by crankcase and crankshaft elasticities. Al-Samieh [13] developed a numerical solution of the Reynolds' equation using Newton- Raphson technique to obtain the film shape and pressure distribution caused by the hydrodynamic viscous action in addition to solvation pressure due to inter-surface forces. The numerical results showed that the effect of changing rolling speed and surface potential on the formation of ultrathin lubricating film thickness. The numerical results showed that the film thickness increase by increasing the rolling speed and surface potential. Mutra et al. [14] proposed an effective optimisation-based identification methodology of bearing stiffness and damping coefficients using the bearing response data. The flexible rotor is initially analysed by a finite element model with nonlinear bearing forces. The dynamic equations of the rotor are solved to obtain the bearing responses in the frequency domain at different operating speeds. The modified particle swarm optimisation is converging faster, and it is taking less computational time.

In the present paper, the effects of bearing steps on the lubrication performance of the main bearings and the probable wear damage have been deliberated. To calculate the bearing lubrication characteristics such as maximum oil film pressure and minimum oil film thickness, elasto-hydrodynamic (EHD) model, which includes a mass conservation algorithm, has been applied. In the current study, in order to calculate the wear volume of main bearings, a model based on the Archard wear model is implemented.

Theory of Elasto-Hydrodynamic and Boundary Lubrication Model

The theory of elasto-hydrodynamic (EHD) model is discussed in the present section. The bearing analysis was carried out using elasto-hydrodynamic model. For the bearing analysis, AVL\Excite® software [15] is a potent tool that was employed for EHD analysis of connecting rod BE bearing in the current work. EHD model is based on the Reynolds equation in Eq. (1) [10] solved in the bearing surface. Equation (1) contains a mass-conserving cavitation model reflected by an additional variable, entitled clearance fill ratio θ. If θ=1, the equation becomes the ordinary Reynolds equation. Reynolds equation is solved via the mass-conserving technique for pressure p in the lubrication region and fill ratio θ in the cavitation region. The fill ratio is defined as the volume fraction filled with oil to the total volume [16]. This parameter serves to model the cavitation effect. Fill ratio equal to one specifies the fully-filled gap, and zero specifies the empty gap [10].

$$\frac{\partial}{\partial x}\left(\frac{\theta h^3}{12\eta}\frac{\partial p}{\partial x}\right)+\frac{\partial}{\partial z}\left(\frac{\theta h^3}{12\eta}\frac{\partial p}{\partial z}\right)=\left(\frac{u_1+u_2}{2}\right)\frac{\partial(\theta h)}{\partial x}+\frac{\partial(\theta h)}{\partial t} \quad (1)$$

The influence of elastic displacement of bearing surface should be considered in EHD analysis. The oil film thickness h is defined as Eq. (2) considering the elastic deformation, shaft misalignment and initial geometrical clearance.

$$h(\beta,z)=C_R-\left(e_x+\alpha_y Z\right)cos\beta-(e_y+\alpha_x Z)sin\beta+\delta(\beta,z) \quad (2)$$

Nodal displacement of the bearing surface is determined by solving the motion equations for the condensed structure of the bearing. Using nodal displacement of the bearing surface along circumferential and radial axes, radial deformation of the bearing surface is acquired. Here, the oil viscosity is defined using Barus' equation:

$$\eta = \eta_0 e^{\alpha p} \tag{3}$$

where, η_0 is the viscosity at the ambient pressure and α is the pressure viscosity coefficient.

If the fully hydrodynamic lubrication regime in bearings was changed to mix lubrication, clearance of bearing drops to an enormously minor level. Therefore, asperities of bearing and shaft surface interact together, subsequently create boundary lubrication conditions. Figure 1 illustrates the asperities of two surfaces that slide on top of each other in boundary lubrication conditions.

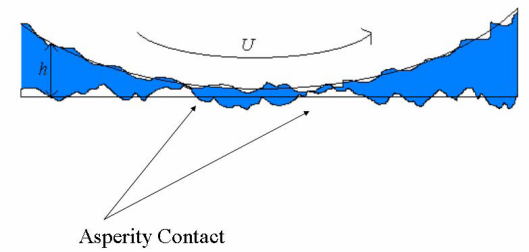

Figure 1. Two rough surfaces in contact with each other in boundary lubrication conditions.

In the mixed-lubrication regime, the boundary lubrication model, according to Greenwood and Tripp [17] is applied for the asperity interaction of two rough surfaces. In this model, two nominally flat surfaces are assumed to have interacted with each other. It is assumed that their asperity curvatures have a fixed radius and asperity heights have a Gaussian distribution. The nominal pressure due to asperities at the region of contact can be defined as below:

$$P_a = KE^* F(\frac{h}{\sigma_s}) \tag{4}$$

where, E^* is composite elastic modulus, K is elastic factor, and F is a parameter depending on the ratio of $\Delta = \frac{h}{\sigma_s}$. σ_s is composite surface asperity height defined as square root of sum of squares of asperity height of two surfaces.

$$\sigma_s = \sqrt{\sigma_1^2 + \sigma_2^2} \tag{5}$$

The elastic factor of the surfaces describes the surface topography as defined in Eq. (6):

$$K = \frac{16\sqrt{2}}{15}\pi(\sigma_s \beta \eta_s)^2 \sqrt{\frac{\sigma_s}{\beta}} \tag{6}$$

where β is the radius at asperity summit, η_S is the surface density peak on each surface and h denotes the nominal clearance between the contacting surfaces. If $\Delta \geq 4$, F will be zero and if $\Delta < 4$, F is expressed as Eq. (7):

$$F\left(\frac{h}{\sigma_s}\right) = 4.4086 * 10^{-5}(4 - \frac{h}{\sigma_s})^{6.804} \tag{7}$$

The elastic behaviour of the rough surfaces is given by the composite elastic modulus and can be expressed as follows:

$$E^* = \frac{1}{\left(\frac{1-v_1^2}{E_1}\right) + \left(\frac{1-v_2^2}{E_2}\right)} \tag{8}$$

where v_1 and v_2 are the Poisson's ratio of the contacting surfaces.

Due to the contact between two mating surfaces, wear has been known as the phenomenon of material removal from surfaces. Practically durability and reliability of most machines are affected by wear failure. IC engine connecting rod works under high load, therefore, sometimes can cause to form a very thin oil film thickness between crankpin and BE bearing. In this kind of circumstances, a fully hydrodynamic lubrication regime changes to mixed lubrication and clearance of bearing drops to an enormously minor level. Therefore, the bearing is subject to wear failure. The wear damage in connecting rod BE bearing can be observed in Figure 2.

Although there are many factors involved in wear failure of bearings especially in running-in, asperity contact stress and minimum oil film thickness are two more important parameters that are used during design process to predict the probability of wear erosion. Hence, it is crucial to study wear during its progress.

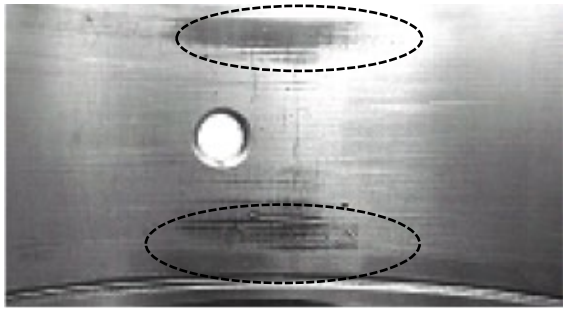

Figure 2. Wear failure in BE bearing.

Mechanism of Wear Failure

Wear is progressive damage at the surface caused by the relative motion of one surface on another material surface. The wear process in bearings is affected by some factors such as sliding speed, load on bearing, oil film thickness, surface finishing of mating surfaces and, most importantly, bearing material. However, the processes involved in lubricated wear are not yet well understood and the effect of above parameters is not easily measurable.

When two contacting surfaces slide against each other, if the oil film thickness is less than the summation of roughness of two surfaces, all asperities in contact with each other break during each cycle. This damage is known as abrasive wear because each asperity slides across several other asperities alongside the opposing surface. Some damages such as sliding wear of lubricated surface (abrasive wear), fatigue of asperities under cyclic loading and subsequent cyclic plastic deformation the following damages may occur under boundary or mixed lubrication regimes which are known as wear. Both fatigue and sliding wear of bearing material should be considered in realistic model of wear. Here, just abrasive wear of the bearing material is evaluated.

When the bearing becomes worn, the thickness amount of minimum oil film is extremely correlated with the surface topology of sliding surfaces. There are many surfaces with different morphologies but the same R_{max} and R_a values. R_{max} is defined as the largest single roughness depth within the evaluation length, and R_a is defined as arithmetical mean surface roughness. By providing only R_{max} and R_a amounts, diverse morphologies are possible for the surface. Only the surface with a very small number of peaks in contact with the sliding surface represents a desirable running surface. As well the surface has some valleys which allow the bearing to retain the oil. Accordingly, the wear model must not only be able to consider the topology of the two sliding surfaces but also be able to consider the changes in the roughness of surfaces during the wear progression.

The bearing area curve (BAC) can be applied as a key parameter to study the wear. A sample of BAC for main bearing is displayed in Figure 3. When the wear damage progresses, the updated BAC of main bearing can be calculated and utilised in the subsequent calculation step. For example, if the sum of surface roughness for the main bearing shell and crankshaft is 2.00 μm, the oil film thickness above this value is related to hydrodynamic lubrication regime and oil film thickness below this value is related to boundary lubrication regime. If lubrication regime goes to boundary lubrication, then that region would be prone to wear damage.

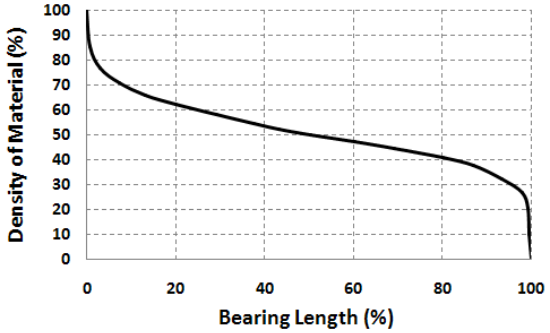

Figure 3. Bearing area curve (BAC) of main bearing.

METHODOLOGY

Using the measurement of the inner diameter of main bearing shells and bearing steps, one can generate the profile of the inner diameter of bearing and then employ the bearing profile in EHD analysis to find the lubrication performance and probable wear and cavitation damage due to bearing shape and bearing step. To reduce the complexity of FE model and computation time, only the crankcase section surrounding the main bearing was modelled. The force and moment were extracted from the global dynamic analysis of the V12 crank train and applied for each main bearing shell.

Modelling

About the modelling approach, it should be noted that the crankshaft flexibility is taken into account. The crankshaft stiffness is altered by a change in Young's modulus of its material. Very flexible crankshaft is denoted as a soft crankshaft, while very stiff crankshaft is denoted as a stiff crankshaft. Soft crankshaft causes the higher crank throw deformation, therefore, leads to force on the crank pin. The force is distributed on adjacent main bearings, and thus the maximum main bearing forces increase. But, the stiff crankshaft leads to lower deformation of the crank throw. In this case, the applied force on the crank throw distributes over all the main bearings, and thus the maximum main bearing forces decrease. Crankshaft flexibility has a major effect on the main bearing force and moment and, therefore, it influences the lubrication performance of engine main bearings. For this reason, the crankshaft flexibility must be considered in the dynamic analysis of the engine crank train. Table 1 presents the different Young's modulus of the material to consider soft, base and stiff crankshaft.

Table 1. Young's modulus of the material to consider soft and stiff crankshaft

Case	Young's Modulus (GPa)
Soft	102.5
Base	205
Stiff	410

Figure 4 shows the schematic representation of the main bearing model in AVL\Excite®. Journal pin was modelled with a stiff solid pin, and then a section of the crankcase was considered as the housing of the main bearing and condensed into entire surface nodes of bearing shell. Figure 5 illustrates the FE mesh of a section of crankcase and EHD joint between the crankcase and main bearing. Translational and rotational movements of the crankcase are fixed using displacement constraints on the symmetry planes. About the FE mesh of crankcase, the bearing shell and two row of elements around them were meshed by linear hexahedral elements, which have higher flexibility in comparison to tetrahedral elements. Therefore, linear hexagonal elements are used for meshing the journal bearings, and their housings and the rest of crankcase are meshed using the linear tetrahedral elements. One main bearing wall is meshed and constrained at the top and side of cutting faces, then its condensed model is generated using sub-structure analysis. The condensed mass and stiffness matrix of one main bearing wall is used for all main bearing walls. To model the engine block, engine or bearing wall elements can be used. For modelling of the simplified crankshaft model, shaft can also be used. To make a connection between the crankshaft and the engine block in the location of main bearing, an EHD connection can be used, which connects the inner surface of the main bearing (engine block) to five nodes of the crankshaft. Engine block and crankshaft journal pin are small motion (SMOT) element. The engine block has very small movements; therefore, it is modelled as SMOT. With the help of the SMOT model, an elastic body with only small general motions is modelled based on a condensed finite element model typically used for engine block structure.

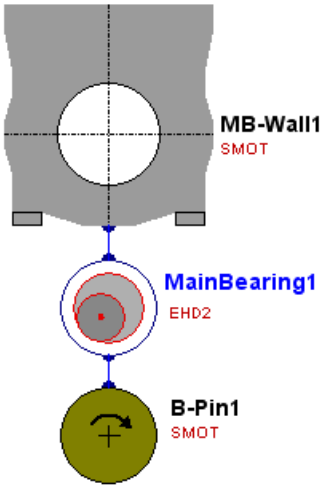

Figure 4. Schematic representation of the main bearing model in AVL\Excite®.

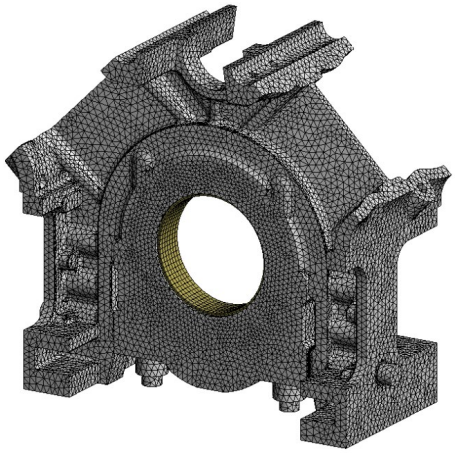

Figure 5. FE mesh of a section of crankcase and EHD joint between the crankcase and main bearing.

Assembled Main Bearing Profile and Bearing Step

Measurement of main bearings comprised of AA, BB, CC, DD and EE bore diameter measurements as well as step measurement at the two banks. Figure 6 illustrates the position of bearing bore measurements. One of the cause roots of the bearing step is the bolt tightening sequence. In this paper, only the results of measured data were used for EHD analysis. Because more explanation about the cause root of bearing step is beyond the scope of this paper, and therefore, it has not been further addressed.

The difference between the A3A3 and E3E3 measures should be approximately equal to the sum of bearing steps of A and B bank side. It should be noted that in all of V12 main bearings except for main bearing No. 4, the step shape is similar to Figure 7. The bearings are numbered from the flywheel side. That is, the bearing closest to the flywheel is called bearing No. 1. During measuring, the deviation of the actual bearing shell profile from the base circle is usually measured just in some positions (e.g. AA, BB, etc.). Therefore, for the main bearings (except for No. 4), a linear average between bearing step sizes (at side A and B) for the upper shell is applied to generate the bearing profile. For the lower shell, a sinusoidal distribution is used. For main bearing No. 4 step shape is like Figure 7(b); a linear average is assumed for both upper and lower shells. Bearing diameter and step measurements were performed for both the front and rear of bearing shell, and consequently, the average of these values was set for computations.

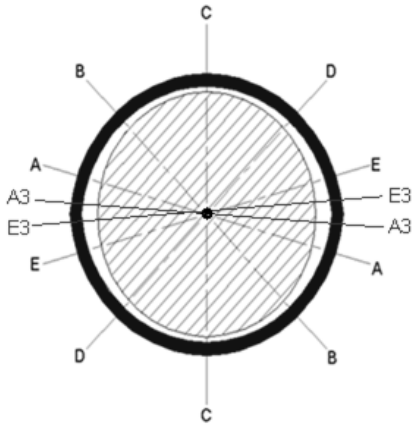

Figure 6. Position of bearing bore measurements.

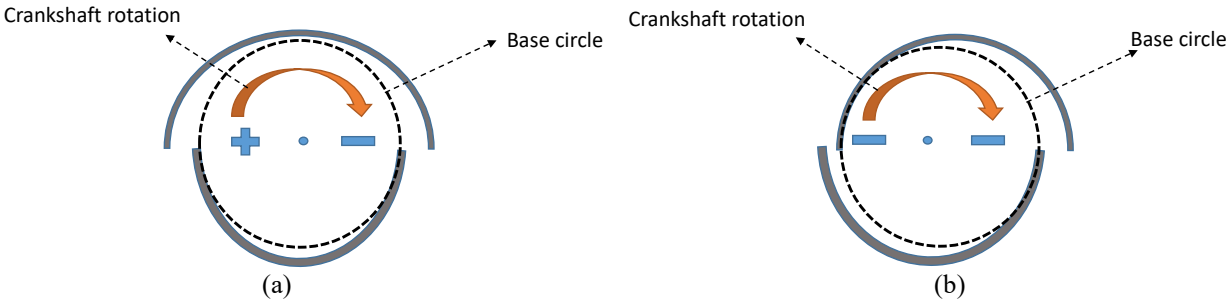

Figure 7. Schematic shape of (a) main bearings with an exception of bearing No. 4, and (b) main bearing No. 4.

RESULTS AND DISCUSSION

EHD Analysis of Main Bearings with Step and Bore Relief

Figure 8 illustrates the exaggerated bearing profile of the main bearing No. 1. Peak oil film pressure (POFP), minimum oil film thickness (MOFT), peak asperity contact pressure (PASP), angular position of MOFT and axial position of MOFT are shown in Figure 9. This amount is almost 3 MPa at 417 degree of crank angle (405° to 450°) in bearing angle of 259 degree, i.e. lower shell A-bank side near the bore relief. Because 3 MPa is relatively low pressure, therefore, low wear damage is predicted in this region for main bearing No. 1. The MOFT that takes place in POFP location is 0.8 μm; therefore, the lubrication regime would be boundary lubrication. In addition, the axial position of MOFT in critical region in terms of wear is at the shell edges.

PASP for main bearing No. 2 is almost 8.5 MPa at 690 degree of crank angle (680° to 710°) in bearing angle of 99 degree, i.e. lower shell B-bank side near bore relief. Because 8.5 MPa is relatively medium pressure, therefore, medium wear damage is predicted in this region. The MOFT is 0.6 μm, therefore, lubrication regime would be boundary lubrication. Also, axial position of MOFT in the critical region for wear damage is at the edge of shells.

PASP for main bearing No.3 is almost 1.2 MPa at 236 degree of crank angle (230° to 245°) in bearing angle of 259 degree, i.e. lower shell A-bank side near bore relief. Because 1.2 MPa is relatively low pressure, therefore low wear damage is predicted in this region for main bearing No.3. The MOFT is 1 μm; therefore, lubrication regime would be boundary lubrication. Also, axial position of MOFT in the critical region for wear damage is at the edge of shells.

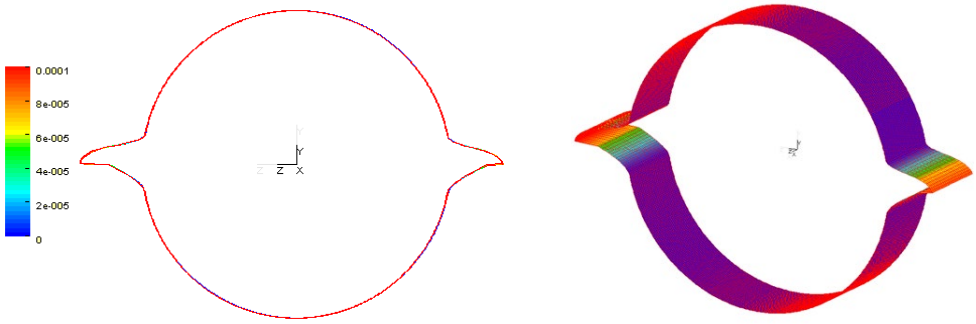

Figure 8. Exaggerated bearing profile of main bearing No. 1 .

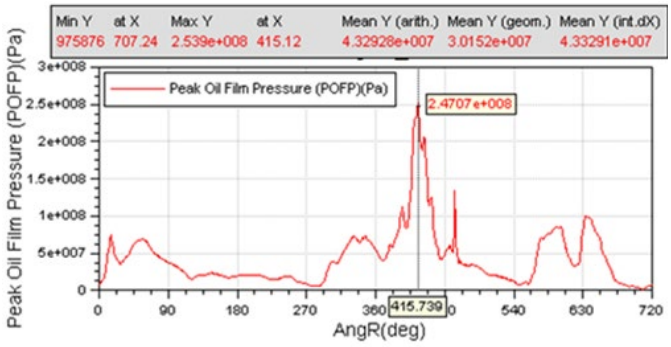

(a) POFP

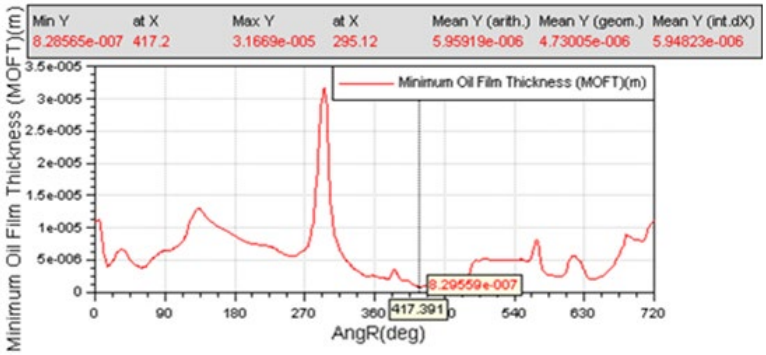

(b) MOFT

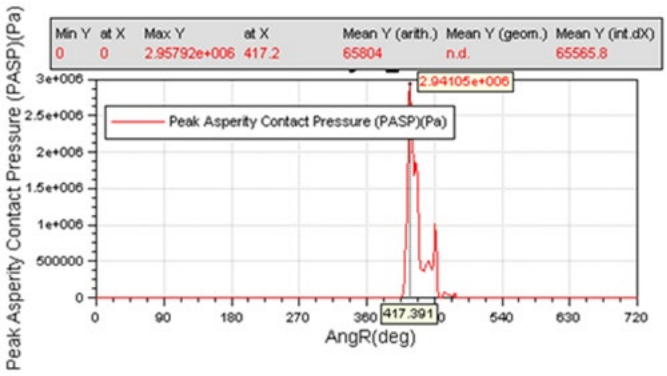

(c) PASP

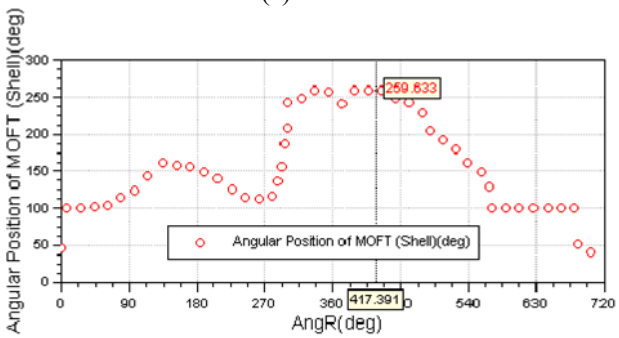

(d) angular position of MOFT

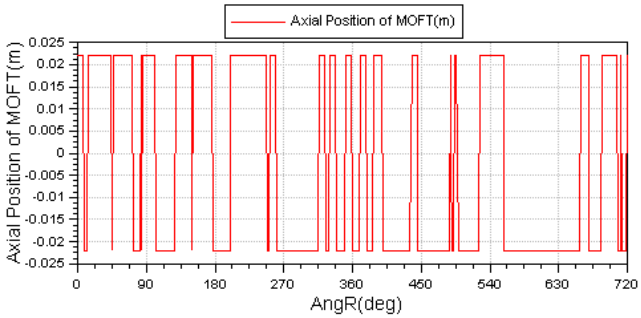

(e) axial position of MOFT

Figure 9. Lubrication analysis results of main bearing No. 1.

Figure 10 illustrates the exaggerated bearing profile of the main bearing No. 4. PASP is shown in Figure 11, which is zero at whole crank angles. Therefore, no wear damage is predicted in main bearing No. 4. The MOFT is 4 μm; is a sufficient oil film thickness not to change the hydrodynamic lubrication regime to mix or boundary lubrication regime.

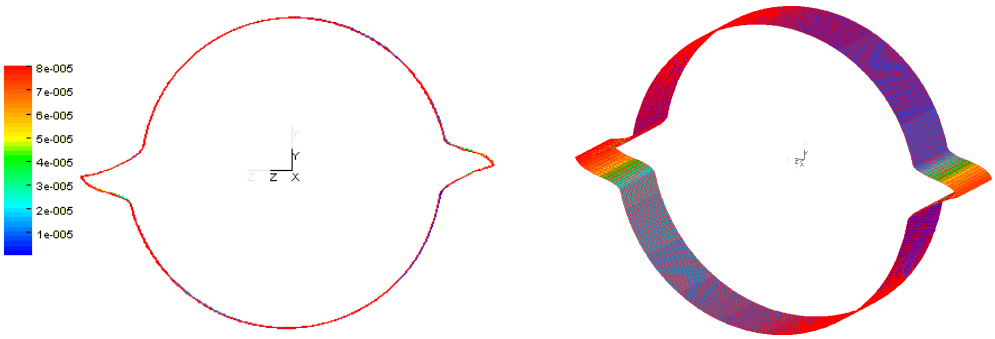

Figure 10. Exaggerated bearing profile of main bearing No. 4.

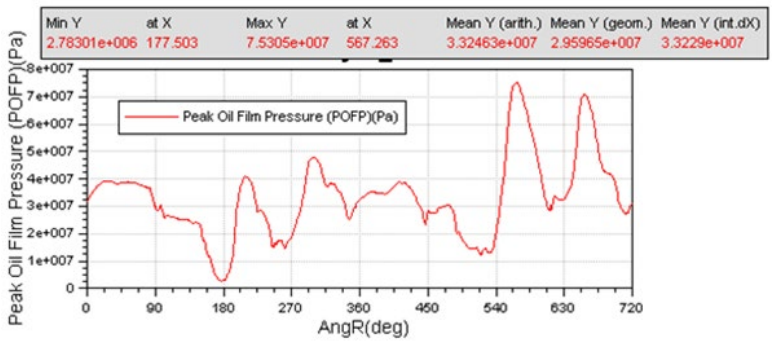

(a) POFP

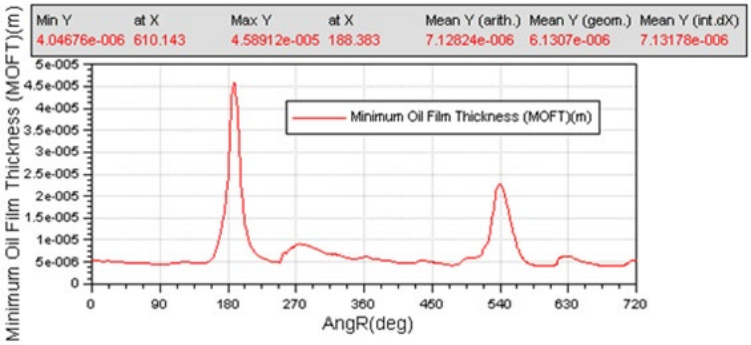

(b) MOFT

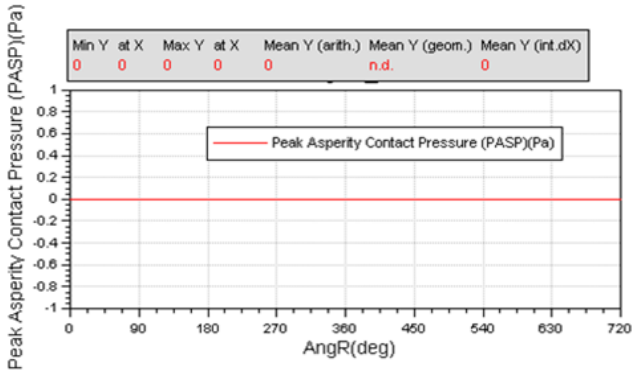

(c) PASP

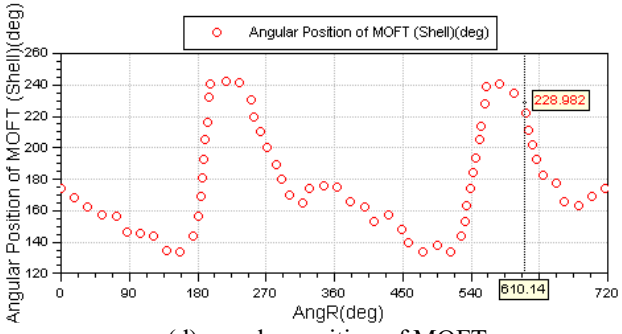

(d) angular position of MOFT

Figure 11. Lubrication analysis results of main bearing No. 4.

In a similar way, for main bearing No.5, the amount of PASP is zero at whole crank angles. Therefore, no wear damage is predicted in main bearing No.5. The MOFT is 3.1 μm that is appropriate oil film thickness not to change the hydrodynamic lubrication regime to mix or boundary lubrication regime. Condition for main bearing No.6 is also the same as No.5. MOFT is 2.1 μm that is sufficient oil film thickness for the hydrodynamic lubrication regime.

For main bearing No.7, the amount of PASP is almost 7.3 MPa at 50 degree of crank angle (35° to 130°) in bearing angle of 259 degree, i.e. lower shell A-bank side near bore relief. 7.3 MPa is relatively medium pressure; therefore, medium wear damage is predicted in this region. The MOFT is 0.7 μm; therefore, lubrication regime would be boundary. Besides, axial position of MOFT in critical region for wear damage is at the edge of shells. Overall, wear damage in bearing No. 1, 2, 3 and 7 happened in bore relief location; for the reason that this location is the first region that the shaft involves to the bearing shell.

EHD Analysis of Main Bearings without Step and Bore Relief

Peak asperity contact pressure in main bearing No.2 is shown in Figure 12. This amount is zero at whole crank angles. Therefore, no wear damage is predicted in main bearing No.2 in case of without step and bore relief. The MOFT is 2.9 μm, which is appropriate oil film thickness not to change the hydrodynamic lubrication regime to mix or boundary lubrication regime. Beforehand, in case of with step and bore relief, medium wear damage was predicted but without step and bore relief, the results do not show any wear. However, in case of without step and with bore relief, high wear damage is also predicted. Consequently, to correctly predict the damages, using EHD model considering bore relief is essential.

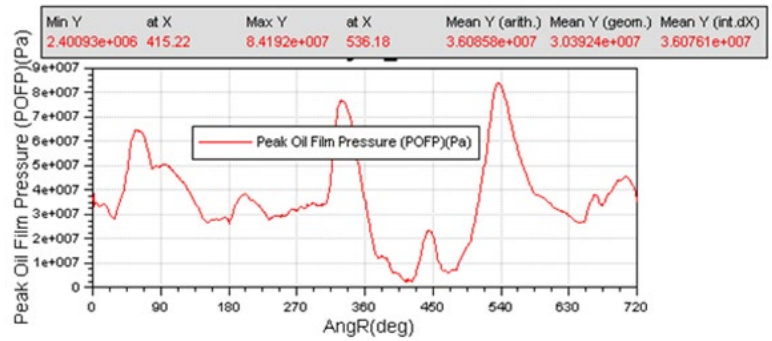

(a) POFP

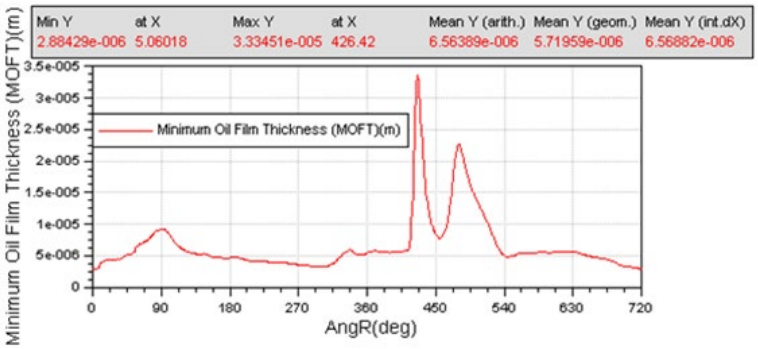

(b) MOFT

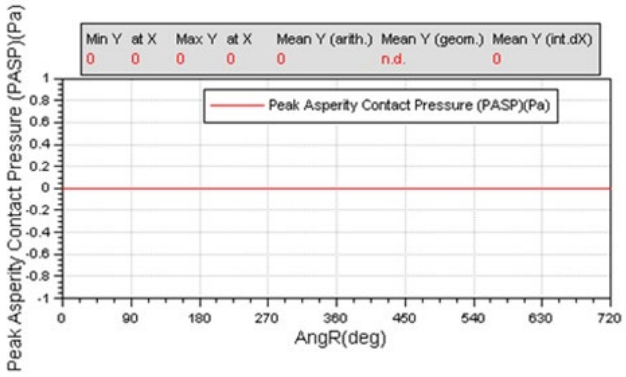

(c) PASP

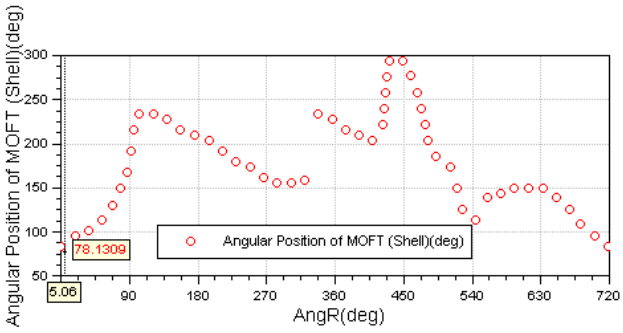

(d) angular position of MOFT

Figure 12. Lubrication analysis results of main bearing No. 2.

PASP in main bearing No. 6 is zero at whole crank angles. Therefore, no wear damage is predicted in main bearing No.6 in case of without step and bore relief. The MOFT is 3.7 μm that is sufficient oil film thickness not to change the hydrodynamic lubrication regime. Main bearing No.6, moreover than the main bearing No.2, has a high dynamic load too; therefore, this main bearing has a critical situation too and must be quietly checked. In both cases, wear damage is not predicted.

PASP in main bearing No. 7 is zero at whole crank angles; therefore, no wear damage is predicted in case of without step and bore relief. The MOFT is 2.7 μm that is appropriate oil film thickness to remain in the hydrodynamic lubrication regime. Main bearing No.7 in case of with step and bore relief shows medium wear damage; therefore, it is checked for the case of without step and bore relief. In both cases, wear damage is not occurred.

EHD Analysis of Main Bearings without Step and with Bore Relief

Peak oil film pressure, minimum oil film thickness, peak asperity contact pressure and angular position of MOFT in main bearing No. 2 are shown in Figure 13. This amount is almost 27.5 MPa at 715 degree of crank angle (700° to 720°) in bearing angle of 72 degree, i.e. upper shell B-bank side. 27.5 MPa is relatively high pressure; therefore, high wear damage is predicted in this region for this main bearing. MOFT that takes place in the POFP is 0.37 μm; therefore, lubrication regime would be as boundary lubrication. Also, axial position of MOFT in critical region for wear damage is at the edge of shells.

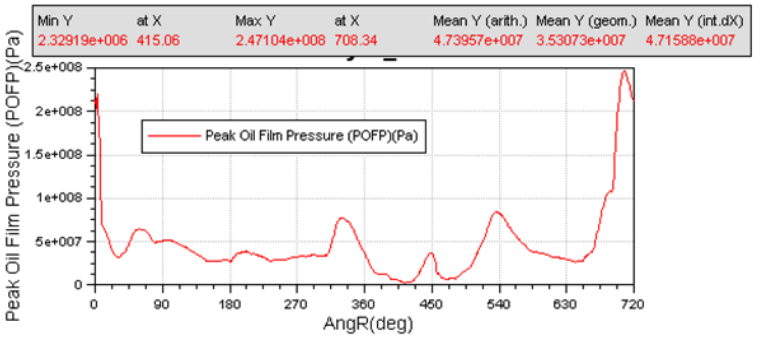

(a) POFP

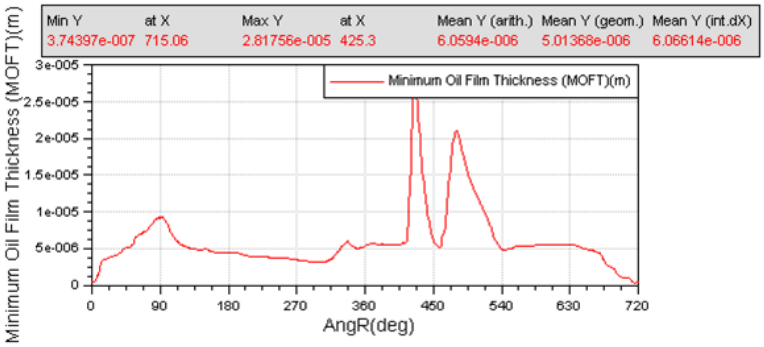

(b) MOFT

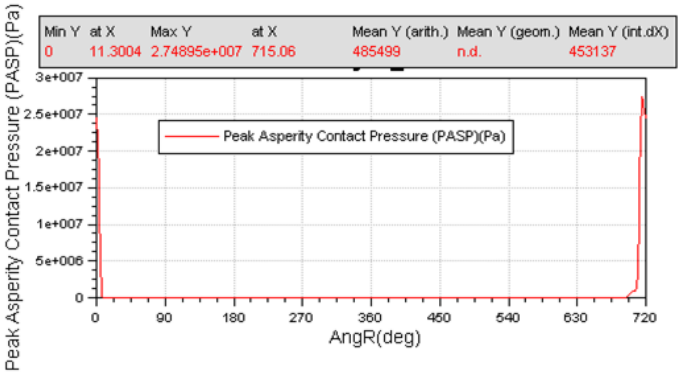

(c) PASP

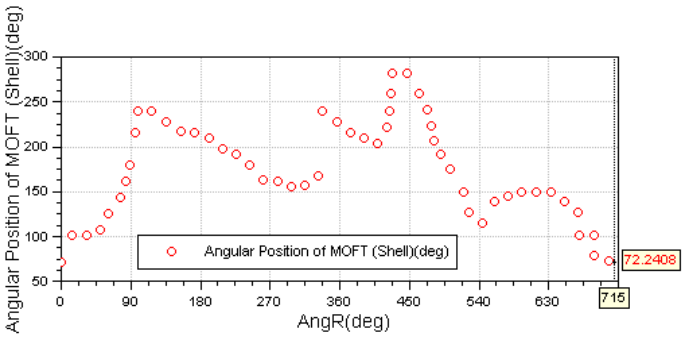

(d) angular position of MOFT

Figure 13. Lubrication analysis results of main bearing No. 2.

HD Analysis of Main Bearings without Step and Bore Relief

Using hydrodynamic (HD) solution, peak asperity contact pressure (PASP) in main bearing No. 2 is obtained as Figure 14. This amount is zero at whole crank angles. Therefore, no wear damage is predicted for that, whereas based on EHD solution, medium wear damage was predicted. Minimum oil film thickness (MOFT) that takes place in POFP location is obtained at 2.3 μm which is sufficient oil film thickness not to change the hydrodynamic lubrication regime to mix or boundary lubrication regime.

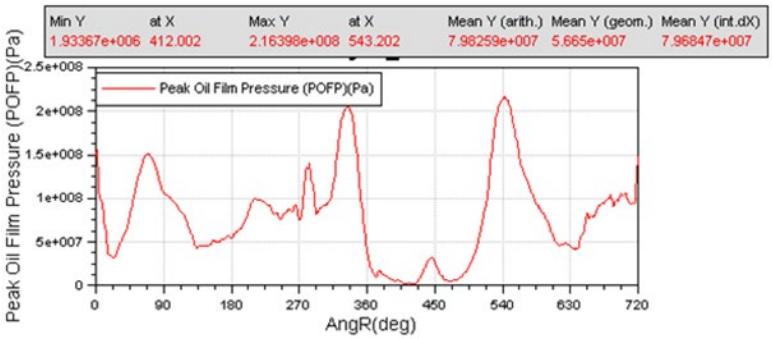

(a) POFP

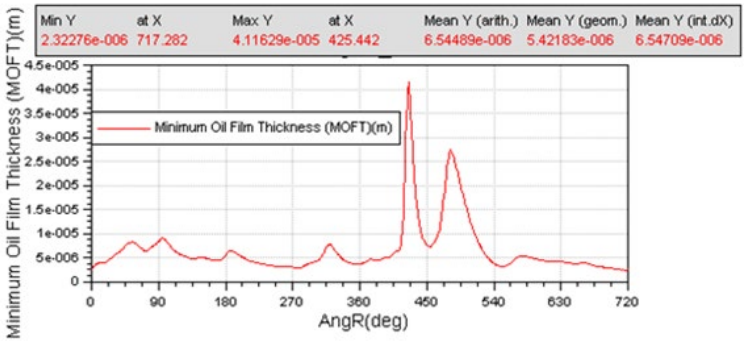

(b) MOFT

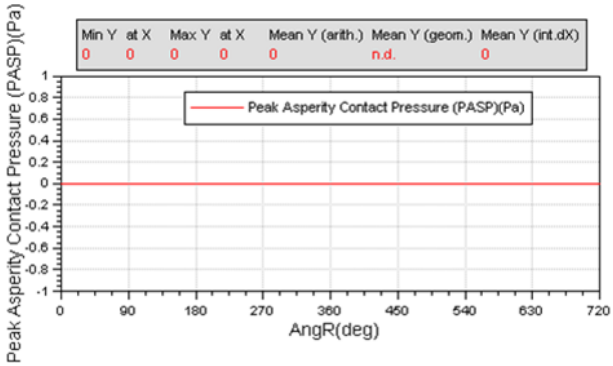

(c) PASP

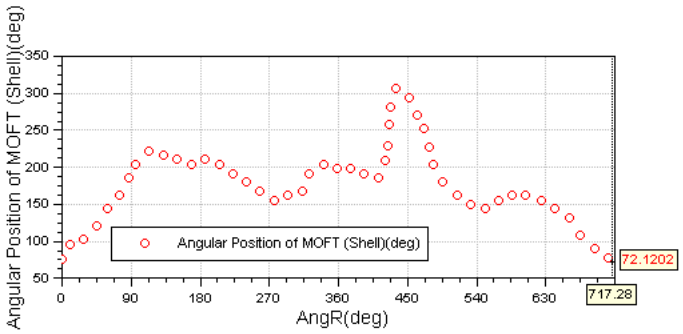

(d) angular position of MOFT

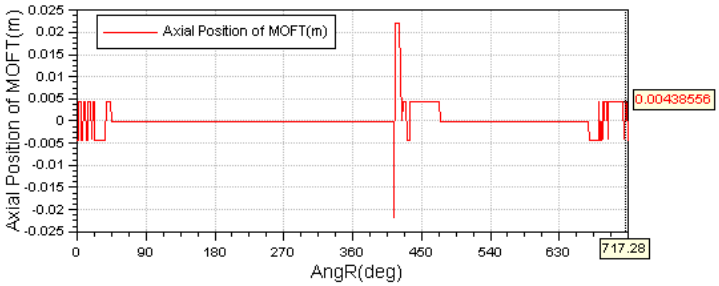

(e) axial position of MOFT

Figure 14. Lubrication analysis results of main bearing No. 2.

This solution shows that HD model presents more optimistic results than EHD model to predict the wear damage. Thus, EHD solution in such cases is strongly recommended. Here, for main bearing No.2, EHD solution predicts wear damage but HD solution not. Based on HD solution, MOFT location is around the middle of axial position, whereas based on EHD solution, MOFT location is at the edge of shells. Table 2 represents the results summary.

Table 2. Summary of the results.

Bearing no.	Step	Relief	HD	EHD	Level of wear damage
1	•	•		•	low
2	•	•		•	medium
				•	not
		•		•	high
			•		not
3	•	•		•	low
4	•	•		•	not
5	•	•		•	not
6				•	not
	•	•		•	not
7	•	•		•	medium
7				•	not

CONCLUSION

Considering real condition (with step and bore relief) in simulation, the main bearing No.1 is not at risk of wear damage. For the main bearing No. 2, because of higher dynamic load, solution was repeated with different considerations, based on both hydrodynamic and elasto-hydrodynamic analyses. Using hydrodynamic analysis, no wear is predicted either without step and bore relief, or with step and bore relief. Based on elasto-hydrodynamic analysis, it is concluded that considering step and bore relief in simulation has a significant effect on the prediction of wear damage. Whereas, hydrodynamic analysis does not make evident for wear damage. Therefore, elasto-hydrodynamic analysis to correctly predict the probable failure is vital. Based on the results, the main bearing No. 2 involved with medium wear damage. The results of elasto-hydrodynamic analysis from main bearing No. 3 show that wear damage in this main bearing isn't dangerous, and for main bearing No. 4, 5 and 6, they do not predict the probability of wear damage. In main bearing No.7, considering step and bore relief in simulation has high importance so that the solution without step and bore relief does not predict the wear, but with step and bore relief predicts medium wear damage.

Consequently, hydrodynamic analysis is not appropriate for the prediction of wear damage in bearings. Therefore, an analysis based on elasto-hydrodynamic model is necessary and important for that. In fact, the prediction of elasto-hydrodynamic model is very proximate to what happens. The reason is that in the hydrodynamic model, the profile of bearing shells and flexibility of housing under dynamic load is not considered, but in the elasto-hydrodynamic, both o are considered and then the clearance between the bearing and its axis is continuously updated.

REFERENCES

[1] Ushijima K, Aoyama S, Kitahara K, et al. A study on engine bearing wear and fatigue using EHL analysis and experimental analysis. SAE paper: 1999-01-1514; 1999.

[2] Archard JF. Contact and rubbing of flat surfaces. Journal of Applied Physics 1953;24(8): pp.981-985.

[3] Wang W, Wong PL. Wear volume determination during running-in for PEHL contacts. Tribology International. 2000;33(7):501–506.

[4] Maas H. Calculations of crankshaft plain bearings. In: ClMAC-Congress, Stockholm, Sweden, pp. 214-222; 1971.

[5] Piraner I, Pflueger C, Bouthier O. Cummins crankshaft and bearing analysis process. In: North American MDI user conference, North Carolina, USA, pp. 98-110; 2002.

[6] Myung-Rae C, Dae-Yoon O, Seung-Hyuk R, Dong-Chul H. Load characteristics of engine main bearing: Comparison between theory and experiment. KSME International Journal 2002;16(8):1095-101.

[7] Pratik K, Pasarkar MD, Thakur AG. Static analysis of crankcase and crankshaft of single cylinder four stroke diesel engine. International Journal on Recent Technologies in Mechanical and Electrical Engineering 2015; 1(5), pp. 1-5.

[8] Rozhdestvensky Y, Khozeniuk N, Surovtsev S. Dynamics and lubrication problem analysis of main bearings for IC engines based on coupling between a crankshaft and a flexible whole engine block. Tribology in Industry 2018;40(1):139-148.

[9] Chamani H, Karimaei H. Lubrication analysis of oil film in main and large eye bearings of a diesel engine using elasto-hydrodynamic analysis. In: Proceedings of the 6th International Conference of Internal Combustion Engines 2009, Tehran, Iran, pp. 1-8; 2009.

[10] Karimaei H, Chamani H. Study of wear and cavitation damages in conrod big end bearing of a heavy duty diesel engine by using elasto-hydrodynamic method. In: Proceedings of the ASME Internal Combustion Engine Division 2009 Fall. Lucerne, Switzerland, pp. 553-565; 2009.

[11] Chamani H, Karimaei H, Bahrami M, Agha Mirsalim SM. Thermo-Elasto-Hydrodynamic (TEHD) analysis of the oil film lubrication in big end bearing of a diesel engine. Journal of Computational an Applied Research in Mechanical Engineering 2015;5(1):13-24.

[12] Karimaei H, Chamani HR. Effect of crankshaft and crankcase material stiffness on load distribution in main bearings. International Journal of Automotive and Mechanical Engineering 2018;15(4):5941-56.

[13] Abd Al-Samieh MF. Formation of ultrathin film between two molecularly smooth surfaces. International Journal of Automotive and Mechanical Engineering 2018;15(1): 4987-5001.

[14] Mutra RR, Srinivas J. An integrated bearing parameter identification approach using a nonlinear optimisation scheme. International Journal of Automotive and Mechanical Engineering 2019;16(1):6245-62.

[15] AVL-Excite®, *Reference Manual*, Version 6.1; AVL List GmbH, Graz, Austria. Retrieved from https://www.avl.com/excite; accessed June, 2004.

[16] Jakobsson B, Floberg L. The finite journal bearing, considering vaporisation. Sweden: Transactions of Chalmers University of Technology 1957; 190(1): 1-116.

[17] Greenwood JA, Tripp JH. The contact of two nominally flat rough surfaces. Proceedings of the Institution of Mechanical Engineers 1970;185(1):625-633.